



Influence of surface effects on the electrostatic separation of zircon and rutile

by J.A. Venter*, M.K.G. Vermaak*, and J.G. Bruwer*

Synopsis

Electrostatic separation is employed in the concentration of zircon and rutile. The zircon concentrate undergoes an acid treatment to remove impurities from the surface of both the zircon and rutile. The purpose of the acid treatment is to increase the difference in the resistivities of the two minerals, thus ensuring the best possible electrostatic separation efficiencies. Previous test work suggested that these impurities are not removed, but only modified; the surface modification seemed more prevalent in the case of the rutile. The resistivity of the rutile changes with pH and thus the electrostatic separation of the rutile is influenced. X-ray photoelectron spectroscopy (XPS) indicates that there is an increase in the OH and adsorbed H₂O concentrations on the rutile surface. XPS also showed significant differential charging on the rutile surface, which indicates that the species on the rutile surface have different resistivities. The zircon particles from the conducting and non-conducting streams have similar resistivities and no major differences in their surface species. Zircon losses during the final electrostatic separation appear not to be due to surface effects, but due to shielding of particles during the separation.

Introduction

Electrostatic separation is the final separation technique employed in the recovery and upgrade of rutile and zircon feedstocks. This dry separation technique is dependent on the difference in resistivities of the rutile and zircon. Even though both minerals have fairly high resistivities (Kelly and Spottiswood, 1989a), the differences in the resistivities are large enough to ensure separation. Of the two minerals rutile has a lower resistivity and is therefore regarded as the conducting mineral. After the initial electrostatic separation between rutile and zircon, the non-conducting zircon concentrate still contains some rutile (approximately 5% by mass). This concentrate is then acid washed to remove impurities, for example, oxides or hydroxides (Gerson, 2006), and thus increasing the difference in the resistivities between the rutile and the zircon. After drying, this zircon-rich stream is again subjected to an electrostatic separation stage to remove as much of the rutile as possible; during this last separation step it is found that

there are zircon losses to the conducting stream. This poses the question whether the acid wash is effective in increasing the difference in resistivity of the two minerals; thus whether it ultimately improves the separation of the minerals.

The initial investigation examined the influence of the neutralization pH of the acid wash on the resistivity of the rutile and zircon (Venter and Vermaak, 2006). It was found that zircon was not very sensitive to the neutralization treatment below a pH of 8 (Figure 1). Above a pH of 8 there was a decrease in the resistivity of zircon. It is not expected that a pH as high as 8 will be reached during neutralization of the acid wash; thus the focus is in the lower pH range. The rutile, on the other hand, showed sensitivity to change in pH over the entire range of pH values (pH 3–10). These results suggested that the lower the pH during pretreatment, the more efficient the subsequent electrostatic separation stage ought to be.

The zircon losses to the conductors also pose the question whether there are some zircon particles that are less resistive than the bulk zircon—zircon particles reporting to the conductor fraction. For this purpose an investigation was performed on the feed stream to the final electrostatic separator stage (after the acid wash) to investigate possible differences in the surface properties of zircon particles reporting to the conductor and the non-conductor fractions (Bruwer *et al.*, 2007). It was found by employing X-ray photoelectron spectroscopy (XPS) and scanning electron microscopy (SEM) that, although not all of the surface impurities were removed during the acid treatment, there are no detectable differences between the zircon in the

* Department of Materials Science and Metallurgical Engineering, University of Pretoria.

© The Southern African Institute of Mining and Metallurgy, 2008. SA ISSN 0038-223X/3.00 + 0.00. This paper was first published at the SAIMM Conference, Heavy Minerals, 10–14 September 2007

Influence of surface effects on the electrostatic separation of zircon and rutile

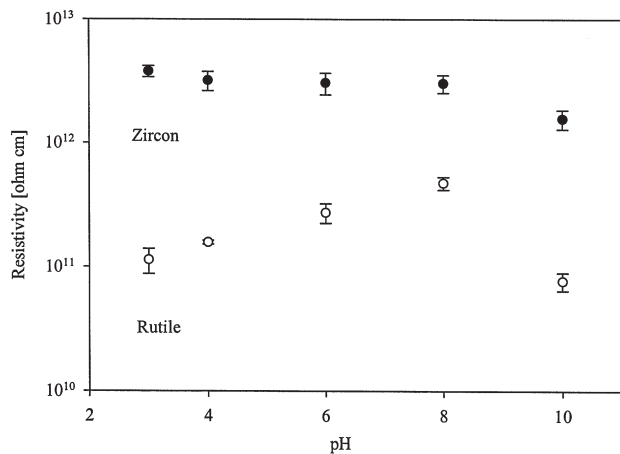


Figure 1—Resistivity of zircon and rutile at 80°C and relative humidity of 80% (at 35°C) after different pH treatments (Venter and Vermaak, 2006)

conductor and non-conductor fractions. These results were verified by use of resistivity measurements that indicated that there is no discernible difference in the resistivities (approximately $2.85 \times 10^{12} \Omega \cdot \text{cm}$ for both) of the zircon in the two streams. Thus it seems that the cause of the zircon losses to the conductors is not material related.

The other point of interest is the sensitivity of the rutile to a change in the pH. From the previous investigation (Venter and Vermaak, 2006) it was apparent that the change in the resistivity is not due to the removal of the surface impurities. The initial XPS investigation indicated that the surface species are, however, modified. Over the years there have been many investigations into the interaction of different species with TiO_2 (Diebold, 2003), most of these on TiO_2 films. From these studies it is evident that rutile can interact with many different species over a wide range of conditions. Rutile also has some catalytic properties, which mean that a wide range of species can adsorb and also be modified on its surface.

The aim of this study is twofold: (i) to investigate if the effect of particle shielding due to machine operating conditions is the cause of the zircon losses, and (ii) to understand the mechanism by which rutile is rendered less resistive during chemical treatments with the aim of optimizing the separation efficiency before the final electrostatic stage.

Experimental

Samples

The same samples used by Bruwer *et al.* (2007) were utilized in the electrostatic separator investigation. The samples originated from Exxaro KZN Sands' treatment plant situated near Empangeni. The samples used for this work were specifically electrostatic separator feed samples; the samples had already gone through the acid and neutralization treatment.

In the case of the rutile investigation the same samples from the previous work (Venter and Vermaak, 2006) were used. The samples also originated from the Exxaro KZN Sands' plant. These samples were acid washed for 2 hours at a pH of 3, H_2SO_4 solution, before they were neutralized at pH

values of 3, 4, 6, 8 and 10 (NaOH used for neutralization), respectively.

Electrostatic separation

The electrostatic separation tests were performed by employing a laboratory Ore Kinetics Corona Stat. All the operating conditions, except the feed rate, were kept constant for all tests. The drum speed was set at 201 rpm and a separation voltage of 24 kV was applied. The feed material temperature was 90°C and the drum of the separator was at 67°C. The environmental conditions were kept constant; ambient temperature of 27.7–28.7°C at a relative humidity of 48–50%. The samples were fed at three different rates, 9 kg/h, 27 kg/h and 100 kg/h, by inserting different perforated feeder plates; the above-mentioned feed rates corresponded to perforated plate with 1.5 mm, 2.5 mm and 4 mm round openings, respectively. The feed rate at 100 kg/h correlates to approximately 4 t/h on an industrial separator, which is closer to the lower limit of operation; thus the 9 kg/h and 27 kg/h mass flow rates are significantly lower than industrial feed rates. The products from the separation were analysed using a Pan Analytical Ex'Pert Pro X-ray spectrometer in theta-theta configuration with Cu radiation, a Ni filter and an X'celerator detector. The samples were scanned from 4° to 90° in variable slit mode. The Rietveldt method using Autoquan software was applied for mineral quantification purposes.

XPS analysis

XPS was performed on the rutile samples neutralized (at pH 4, 8 and 10) after the acid pretreatment step at pH 3. A Physical Electronics model 5400 equipped with an Al/Mg dual X-ray source and an Al monochromator was used for the XPS analysis. A Jeol JSM 6300 with a Noran EDS system operated at an accelerating voltage of 20 kV was used for the SEM analysis. The surface charge neutralizer was also employed at a current of 25 mA.

Results and discussion

Electrostatic separation

The focus of the first part of the experimental work was to investigate the effect of flow rate on the zircon losses to the conductor stream. From Figure 2 it is quite evident that the initial increase in feed rate from 9 kg/h to 27 kg/h did not cause a significant increase in the zircon losses to the conductors. However, when the feed rate was increased to 100 kg/h the zircon recovery (losses) to the conductors increased by a factor of four. The cumulative mass pull indicates that the bulk sample has a similar behaviour to an increase in the feed rate, thus irrespective of the mineral. This indicates that some of the zircon particles are not separated only due to its physical properties and that the effect is increased by an increase in the feed rate. The cause of this misplacement is probably due to some of the zircon particles being shielded from the drum by some conducting particles and thus will report with the conductors. As the bed depth on the drum increases more particles are shielded from the drum. Ideal electrostatic separation would be possible if the bed depth were only a single particle deep. This is, however, not practical for industrial purposes. Thus some losses due to



Influence of surface effects on the electrostatic separation of zircon and rutile

machine operation will always be expected; multi-stage processing is undertaken to minimize losses. This, however, confirms the findings by Bruwer *et al.* (2007) that misplacement of zircon can occur even if there is no significant difference between the zircon in the conductor and in the non-conductor fractions.

Figure 2 also indicates that for the lower feed rates, especially 9 kg/h, the bulk of the zircon is recovered to middlings 3 (middlings stream closest to non-conductor stream). In contrast, at the high feed rate, 100 kg/h, the bulk of the zircon reaches the brush on the drum and is deposited into the non-conductor stream. The particles that leave the drum into the middlings 3 stream are due to the change in the force balance across the particle (Figure 3) (Kelly and Spottiswood, 1989b).

The forces acting on a particle on the drum are the following:

- F_e – Force due to electrical field
- F_c – Centrifugal force
- F_f – Frictional force
- F_g – Gravitational force
- F_i – Image force

Usually the frictional force, F_f , is so small relative to the other forces that it can be ignored. At the point where the middlings 3 stream leaves the drum the electrical field's influence is very small and thus F_e can also be ignored. The gravitational force is strongly dependent on the diameter of the particle, $F_g \propto d^3$ (where d is in metres). Thus in this current investigation where the average particle size is approximately 150 μm F_g is negligibly small. This means that at the point of release the major forces on the particles are the centrifugal force (F_c) countered by the image force (F_i). The image force is due to the attraction of the charged particle to the grounded surface (drum); it is equivalent to the attraction between the charged particle and its mirror behind the surface. The resulting force from the centrifugal and image forces can be characterized by a pinning factor F_p ; where

$$F_p = \frac{F_i}{F_c} \quad [1]$$

and

$$F_p = \frac{6Q^2}{\pi\rho_s K_r d^5 R \omega^2} \quad [2]$$

- Where Q = total charge (C)
- ρ_s = particle density (kg/m^3)
- K_r = constant
- d = particle diameter (m)
- R = drum radius (m)
- ω = drum angular velocity (rad/s)

As long as this ratio is larger than one, the particle is pinned to the drum. It is clear from Equation [2] that the pinning force is dependent on the charge of the particle. The discharging of the particle is time dependent, as can be seen in Figure 4 (Kelly and Spottiswood, 1989b). It is evident from Figure 4 that $Q \propto e^{-kt}$.

In the current investigation it is clear that at low feed rates (9 kg/h) ideal single particle bed conditions are approached. Thus each particle is directly in contact with the

grounded surface. This means that the discharging of the particles is only dependent on their own charge and thus by the time the drum reaches the middlings 3 position $F_p < 1$; thus the particle is no longer pinned to the drum. In the case of the high feed rate (100 kg/h) there are layers of particles on top of each other. This causes a decrease in the discharging time due to non-conductors that need to discharge through other non-conductors. This ultimately causes the inner particles to be pinned for longer times to the drum. This is the cause of misplaced conductors to the non-conductors.

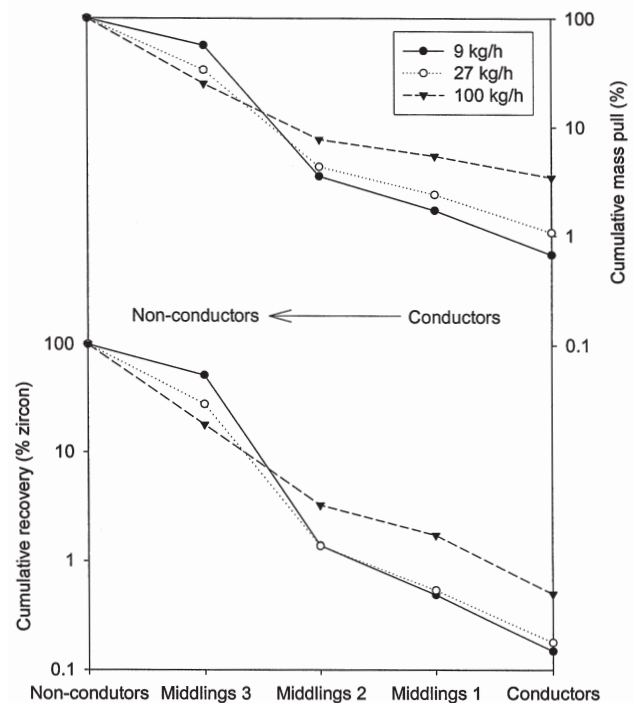


Figure 2—Mass pull and zircon recoveries to the different streams for electrostatic separation at 24 kV for different feed rates: 9 kg/h, 27 kg/h and 100 kg/h

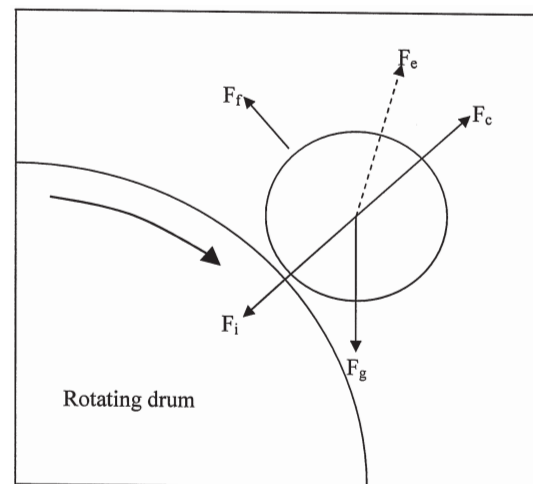
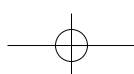
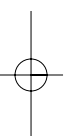


Figure 3—Forces acting on a particle in an electrostatic separator (Kelly and Spottiswood, 1989b)



Influence of surface effects on the electrostatic separation of zircon and rutile

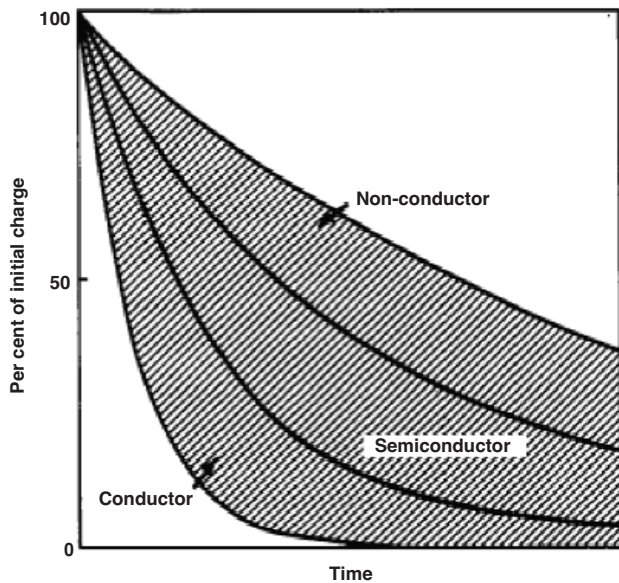


Figure 4—Particle discharging curves (Kelly and Spottiswood, 1989b)

It can be seen that $Q \propto \omega$ for the same pinning force with all the other variables staying constant. Thus it should be possible in the case where the particles are discharging faster to increase the drum speed without significant increase of misplaced non-conductors as long as the increased F_c is not larger than the initial F_i .

XPS analysis

Figure 5 shows the XPS spectra of the rutile samples neutralized at different pH values. The spectra indicated the presence of the same elemental species—Fe, O, Ti, C, Si and Al—on the surface of the rutile sample. Quantitative analysis indicated that there were no significant changes in the elemental species concentrations between the samples. It is, however, evident that there are major changes in the recorded peak shapes. This is quite visible for the O 1s and C 1s peaks. Multiplexes were recorded for all the identified elements. The majority of the carbon on the surface is due to hydrocarbon adsorption from the atmosphere (contaminants in the atmosphere). In Figure 6 the C 1s, recorded without the neutralization of the surface charge, shows two very distinct peaks. Normally one would expect only a single fairly sharp peak at approximately 285 eV (Chastain, 1992). That the peaks are present at higher binding energies is due to charge build-up on the surface. Rutile has a fairly high resistivity, thus the charge build-up is quite significant. Only a single peak, at approximately 285 eV, is visible after the sample's surface charge was neutralized. The disappearance of the one peak indicates that there are areas with different resistivities on the rutile surface, this causes differential charging. After neutralization the surface has a uniform charge and thus the one peak will shift more significantly. Differential charging was observed for the peaks of all the elements except the Fe. In the case of the Fe only a shift in the Fe 2p_{3/2} and 2p_{1/2} and not a change in the shape or number of peaks could be detected after neutralization. This indicates that the Fe is present in only one of the measured surface areas; most probably it is a small amount of Fe present in the rutile itself.

The most information can usually be determined from XPS analysis by the analysis of the O 1s peak. From Figure 7 the first important observation is the decrease and ultimate disappearance of the Al₂O₃ species. One would expect the Al₂O₃ species to be stable at a pH of 4 (can dissolve as Al³⁺ at pH < 4), but possibly dissolve at high pH values. This is precisely what is observed; with the most Al₂O₃ present at pH 4 and no Al₂O₃ present at pH 10. It is important to note that the amount of the Al₂O₃ species does not significantly contribute to the overall amount of Al present on the surface. Further, it is apparent from the analysis that there are only three, possibly four, oxide species present in all the samples (excluding the Al₂O₃ species). The analysis indicates the major species present are TiO₂, SiO₂ and H₂O. The SiO₂ and OH peaks coincide, which makes it difficult to distinguish between the two species. However, SiO₂ should be relatively stable over the whole pH range of the investigation. The ability of rutile to adsorb OH is known, especially during the photocatalytic reaction between rutile and water in alkaline solutions (Jensen *et al.*, 2005). At a low

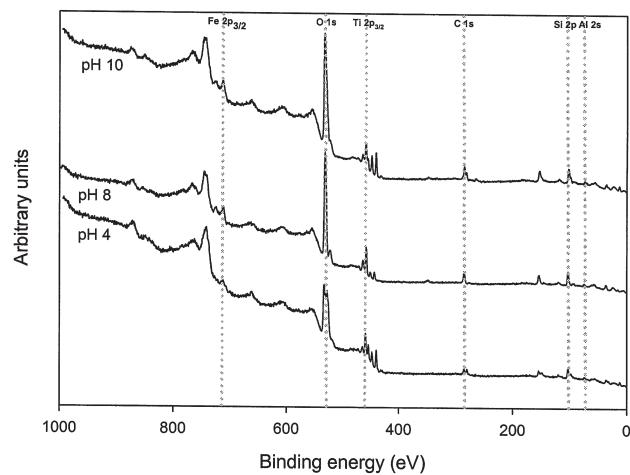


Figure 5—XPS survey spectra of the rutile surfaces after neutralization at pH 4, 8 and 10

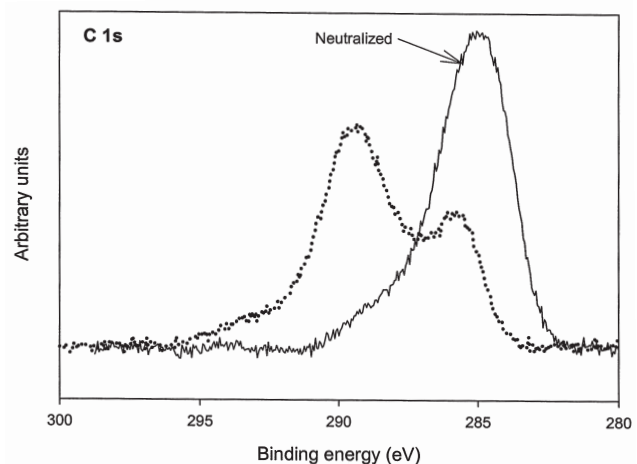


Figure 6—XPS multiplex of the C 1s region of the rutile surface of the pH 10 sample; before and after neutralization of the surface charge

Influence of surface effects on the electrostatic separation of zircon and rutile

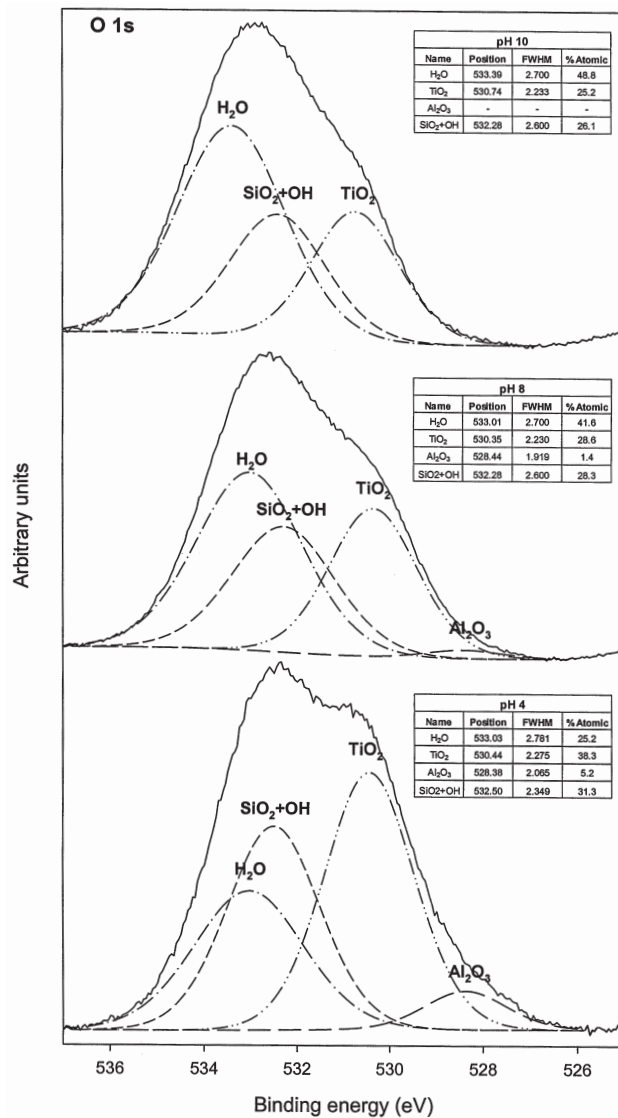


Figure 7—XPS multiplexes of the O 1s region for rutile samples treated at pH 4, 8 and 10

pH there should be very little OH species present, thus one expects that at a pH of 4 the SiO₂ + OH peak will probably consist of only SiO₂. As the pH increases the SiO₂ + OH peak increases, indicating that the concentration of OH on the surface increases. This can be clearly seen in the ratio between TiO₂ and SiO₂ + OH concentrations (Table I). This OH species should be due to reprecipitation on the rutile surface, since all samples were first washed at a pH of 3, dried and then neutralized at a pH of 4, 8 and 10, respectively. The other significant change observed is the increase in the amount of H₂O observed. As the pH increases the H₂O concentration also increases.

From these XPS results it is possible to see that the lower resistivity of the pH 4 sample relative to the pH 8 sample is probably due to the lower OH concentration and thus 'cleaner' surface. On the other side of the pH spectra there is also a decrease in the resistivity relative to pH 8. Even though there is a further increase in the OH species concentration, there is also a significant increase in the adsorbed water. This increased concentration of water is probably due

to the increased OH concentration that also increases the hydrophilicity of the rutile. (Note: as the OH concentration increases the H₂O concentration increases.) There is a strong correlation between humidity and resistivity (Kelly and Spottiswood, 1989b), thus also between H₂O present and resistivity. The correlation can be expressed as follows:

$$\log \frac{1}{\sigma_r} \propto H \quad [3]$$

where σ_r = relative resistivity
 H = relative humidity

Thus the adsorbed water renders the rutile less resistive. It is interesting to note that the moisture content measurements (Figure 8) performed during the resistivity measurements (Venter and Vermaak, 2006) do not indicate a significant change over the pH range. These measurements were done for the bulk sample and thus include the adsorbed water and not just the adsorbed water. Even though there are significant differences in the concentration of the adsorbed water on the different rutile samples, the overall concentration is insignificantly lower than the adsorbed water concentration during the bulk measurements.

Conclusions

From this investigation it is apparent that the losses in the zircon circuit are possibly due to inherent separation inefficiencies as there is no significant difference between the

Table I

Ratio of TiO₂ to SiO₂+OH and H₂O

pH	% Atomic		Ratio		
	TiO ₂	SiO ₂ + OH	H ₂ O	TiO ₂ : SiO ₂ + OH	TiO ₂ : H ₂ O
4	38.3	31.3	25.2	0.82	0.66
8	28.6	28.3	41.6	0.99	1.45
10	25.2	26.1	48.8	1.04	1.94

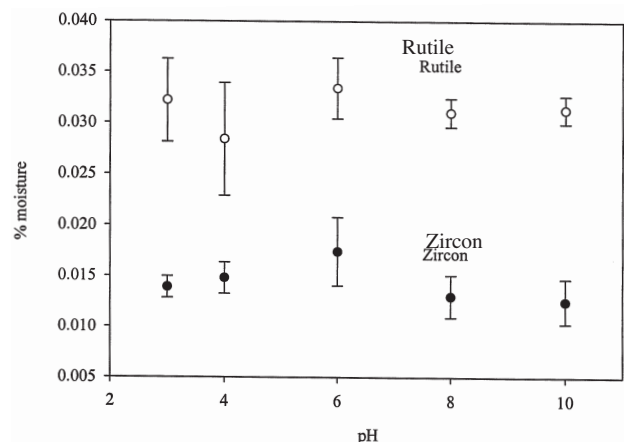


Figure 8—Moisture content of rutile and zircon samples at 80°C and relative humidity of 80% at 35°C for different pH treatments (Venter and Vermaak, 2006)

Influence of surface effects on the electrostatic separation of zircon and rutile

surface properties of zircon in the non-conductor or conductor streams. It is possible to minimize these by optimizing the machine parameters. However, the problem is that for the optimum efficiency one requires very low feed rates, which are not practical. To solve the problems around the zircon concentrator one could possibly try and increase the separation efficiency in the previous step by ensuring the highest possible difference in resistivities between the rutile and the zircon— although in the end the inherent losses will still be the limiting factor. Another possibility is to rather use another type of concentrator—for example reverse flotation (Mao *et al.*, 1994), since it is a very useful method for concentrating low grade ores.

In the case of the rutile it was found that the presence of OH is responsible for the change in the resistivity of the rutile. The OH concentration on the rutile increases with an increase in the pH. Initially this increased concentration increases the resistivity of the rutile, but it also increases the concentration of the adsorbed H₂O on the surface. At high pH values the H₂O concentration is the determining factor for the resistivity and thus the resistivity decreases again. This study also indicated the importance of XPS investigations concerning electrostatic separation, where the outermost surface layers can play a very significant role.

References

- BRUWER, J.G., VERMAAK, M.K.G., and VENTER, J.A. Zircon surface characterization, *The Journal of the Southern African Institute of Mining and Metallurgy*, 2007, vol. 104, no. 4, pp. 237–239.
- CHASTAIN, J. (ed.), *Handbook of X-ray photoelectron spectroscopy*, Perkin-Elmer Corporation, Physical Electronics Division, Eden Prairie, Minnesota, USA, 1992, pp. 40–41.
- DIEBOLD, U. The surface science of titanium dioxide, *Surface Science Reports*, 2003, vol. 48, pp. 53–229.
- GERSON, A. Zircon surface coatings, *ACeSSS*, University of South Australia, 2006
- JENSEN, H., SOLOVIEV, A., LI, Z., and SØGAARD, E.G. XPS and FTIR investigation of the surface properties of different prepared titania nano-powders, *Applied Surface Science*, 2005, vol. 246, pp. 239–249.
- KELLY, E.G. and SPOTTISWOOD, D.J. The theory of electrostatic separation: A review part I. Fundamentals, *Minerals Engineering*, 1989a, vol. 2, no.1, pp. 33–46.
- KELLY, E.G. AND SPOTTISWOOD, D.J. The theory of electrostatic separation: A review part III. The separation of particles, *Minerals Engineering*, 1989b, vol. 2, no. 2, pp. 337–349.
- MAO, M., FORNASIERO, D., RALSTON, J., SMART, R., ST. C., and SOBIEK, S. Electrochemistry of the zircon-water interface, *Colloids and Surfaces A: Physicochemical and Engineering Aspects*, 1994, vol. 84, pp. 37–49.
- VENTER, J.A. and VERMAAK, M.K.G. The influence of pH on the electrostatic separation of rutile and zircon, *XXIII International Mineral Processing Congress*, Istanbul, 2006, pp. 304–309. ◆

LEADERS IN STAINLESS STEEL FABRICATION

WE'RE NOT MINERS

WE'RE NOT MINERALS PRODUCERS



BUT WE CAN DO STAINLESS.

With 50 years of commitment to quality and delivery for clients in Mining, Pulp and Paper, Textiles, Petrochemical and Sugar, Styria can rightfully say: "We can do stainless."

A proud supplier of Pressure vessels, Storage tanks, Cyclones, Hoppers, Chutes and other fabrications.

A Focus on Stainless Steel

Styria Engineering (Pty) Ltd
132 Terrace Road Edenvale PO Box 9748 Edenglen 1613
Tel: (011) 452-1150 Fax: (011) 452-2450 E-mail: styria@netactive.co.za

METQUIP
SPECIALISED EQUIPMENT COMPANIES



Styria
STAINLESS STEEL
FABRICATION